

ELECTRON SPIN RESONANCE STUDIES OF ELECTRON  
IRRADIATED ALUMINIUM OXIDES

J. Reyes L.\*

Programa de Aplicaciones Industriales de la Radiación,  
Comisión Nacional de Energía Nuclear

S.A. Reyes L.

Instituto de Física, Universidad Nacional de México

(Recibido: junio 23, 1969)

RESUMEN

*Se estudia la concentración, en relación con la dosis, de los centros paramagnéticos inducidos por la irradiación con electrones de 1.0 MeV de energía, en polvo de cuatro tipos de catalizadores formados a base de óxido de aluminio, por medio de la resonancia del espín electrónico. La variación de la concentración con el tiempo fue determinada a diversas temperaturas de almacenamiento y el promedio de las energías de activación para los procesos totales de recombinación térmica de los centros fue determinado para los intervalos de temperatura, de 20 a 100 y de 100 a 150°C.*

---

\* Instituto de Física, Universidad Nacional Autónoma de México.

## ABSTRACT

*The relation between dose and the concentration of paramagnetic species induced by 1.0 MeV electron irradiation in powders of four types of aluminium oxides catalysts, was studied by the electron-spin resonance technique. The variation of the concentration with time was determined for several temperatures of storage, and the mean activation energies for the total processes of thermal annealing of the centres were determined in temperature intervals from 20 to 100 and 100 to 150° C.*

## INTRODUCTION

**1. Heterogeneous Radiation Catalysis in aluminium oxide catalysts.**

Many chemical reactions are known to proceed by the action of radiation on absorbed substances on aluminium oxide catalysts. The radiolytical yield  $G$  of several reaction products exceeds the respective values for the homogeneous radiolysis of those substances, as can be seen in some examples presented in table 1. There,  $G_{\text{het}}$  is the yield calculated with respect to the energy taken up by both the substance and the sorbent.  $G_{\text{hom}}$  is the yield of the radiolysis in the homogeneous gas, liquid or solid phase. In some cases the  $G_{\text{het}}/G_{\text{hom}}$  ratio is close to unity and some times even higher. This seems to show that radiation energy is sometimes more efficient when taken up by the sorbent than by the reacting substance. Thus, energy absorbed in the solid is capable of decomposing the substance absorbed on its surface and the phenomenon can be termed energy transfer. Then, as pointed out by several authors, the phenomenon of radiation-induced catalysis may be connected with ionization processes in the solid and with the trapped non-equilibrium charge carriers. There seems to be some evidence for interaction of such species with absorbed molecules. Perhaps transfer of energy may occur mainly by recombination of non-equilibrium charge carriers.

Table 1.- Radiolytical yields for several products from reactions induced by ionizing radiations in substances absorbed in aluminium oxide catalyst compared with those of the homogeneous radiolysis.

Substance	Product (s)	G value		$G_{\text{het}}/G_{\text{hom}}$	References
		heterogeneous	homogeneous		
$\text{N}_2 + \text{H}_2$	$\text{NH}_3$	2.4-1.0	0.7	3.4-1.4	1
$\text{C}_2\text{H}_4 + \text{CO}_2$	Carbonic acids	$5 \times 10^3$	$10^2$	50	2
$\text{C}_2\text{H}_4 + \text{NH}_3$	Amines	$10^4$	$10^3$	10	2
$\text{CO}_2$	CO	0.11	0.02	5	3
$\text{CH}_3\text{OH}$	$\text{H}_2$	65.5	5.1	12.8	4
	$\text{CH}_2\text{O}$	26.6	1.6	16.6	4
	$(\text{CH}_2\text{OH})_2$	37.7	3.9	9.6	4
$\text{c-C}_6\text{H}_{12}$	$\text{H}_2$	0.19	5.5	0.03	5, 6

## 2. ESR of irradiated aluminium oxide catalysts.

Trapped non-equilibrium charge carriers can be detected by electron spin resonance (ESR). The paramagnetic species induced by ionizing radiation in aluminium-oxide catalysts have been studied by several authors<sup>7-12</sup>. Different paramagnetic species have been found, depending on the kind of catalyst, type of ionizing radiation used, irradiation temperature and pre-treatment temperature of the catalyst.

## 3. Materials

The following materials were used without any pre-treatment:

Activated basic aluminium oxide (Merck, 1076) (BAO)

Activated neutral aluminium oxide (Merck, 1077) (NAO)

Activated acid aluminium oxide (Merck, 1078) (AAO)

Activated alumina (A-1, Ferro Enamel de México, S.A.) (AA)

X-ray spectrographic qualitative determination shows traces of several elements, with relative abundances given in table 2. These traces are supposed to come from the industrial preparation of the oxides but no information has been received from the company to date.

## 4. Irradiation techniques and dosimetry

Using the Van de Graaff accelerator at the Instituto de Física, UNAM, the samples were irradiated with 1.0 MeV electrons, in air, at room temperature, in a 1 mm thick layer, in order to obtain good dose distribution. The dose rate for the sample  $((D.R.)_S)$  was 545 rad/sec, determined by using the relation

$$(D.R.)_S = \frac{m^S_s}{m^S_d} (D.R.)_d \quad (1)$$

Table 2.- Relative abundances of several elements determined by X-ray spectrographic qualitative analysis.

Catalyst	Components (%)			
	> 10	0.1 - 1	0.01 - 0.1	0.01
BAO	Al	Na	Si, Fe, V	Cr, Ga, Ca, Mg, Cu, Ti
NAO	Al	-	Na, Si, V	Ge, Fe, Ca, Mg, Cu, Ti
AAO	Al	-	V, Si	Fe, Ga, Ca, Mg, Cu, Ti
AA	Al	Na	Fe, Si, V	Ga, Ca, Mg, Cu, Ti

Table 3.- Line width  $\Delta H$  and g values for the paramagnetic resonance line induced by electron irradiation in aluminium oxide catalysts.

Catalyst	g values	Line width $\Delta H$ (gauss)
BAO	$2.0126 \pm 0.006$	42.0
NAO	$2.0124 \pm 0.006$	46.5
AAO	$2.0130 \pm 0.006$	41.7
AA	$2.0273 \pm 0.006$	-

where  $(D.R.)_d$  is the dose rate for the cobalt-activated borosilicate glass powder, used as dosimeter<sup>13</sup> and irradiated under the same conditions as the samples. The stopping-power fraction has the value 0.970, calculated from the formal definition, using the following data: effective atomic number of aluminium oxide  $Z = 9.337$ ; mean excitation potential,  $I = 126.9$  eV; and mean density,  $\rho = 2.266$  g/cc. The data are taken from Nelms<sup>14</sup> and Henricksen<sup>15</sup>.

### 5. ESR determinations

ESR determinations were made at different temperatures, using the Varian 4502-15 EPR spectrometer, at the Instituto de Física, UNAM, operating at a microwave frequency in the X-band near 9.4 GHz with 100 KHz field modulation. A temperature-variable controller was used to maintain the sample in the spectrometer cavity at a fixed temperature in order to study the temperature annealing of the paramagnetic species.

## RESULTS AND DISCUSSION

After powder of the catalysts has been exposed to electron irradiation, a single, asymmetric paramagnetic resonance line is observed with line width  $\Delta H$  and  $g$  values shown in table 3. The growth behaviour of the electron-induced ESR line in aluminium oxide (figure 1) as well as the low-photon energy required to cause the ESR absorption, suggests either that the resonance is due to ionization which takes place at the site of a structural defect, or that the resonance is associated with impurities in the crystal that form the powder.

From fig. 1, it is possible to see that the concentration of paramagnetic species for a fixed dose depends on the catalysts. The higher concentration in the acid oxide is due to the presence of an additional structural defect coming from the industrial treatment or due to impurities. From the data obtained by X-ray spectrography we are led to assume that it is due to the first cause.

In the case of activated alumina, an ESR line is observed without irradi-

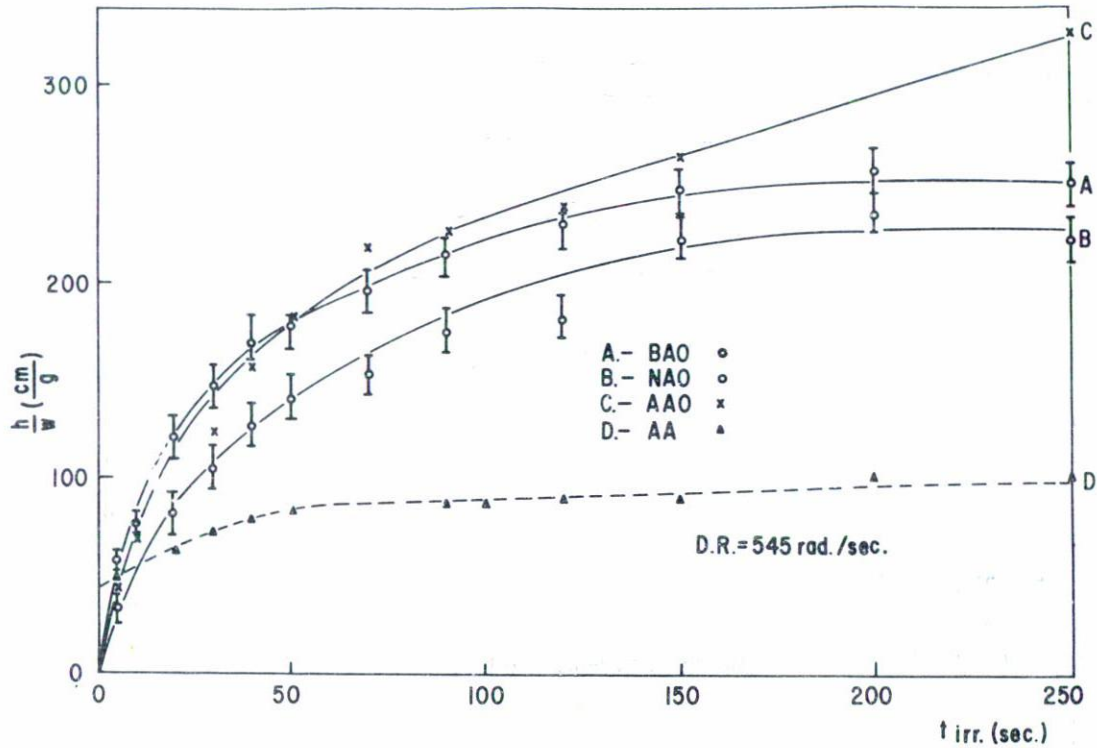


Fig. 1 Growth dose behaviour of the electron-induced ESR line in aluminium oxide catalysts.  $(b/w)$  represents the first derivative ESR line peak to peak height per mass unit. D.R. is the dose rate.

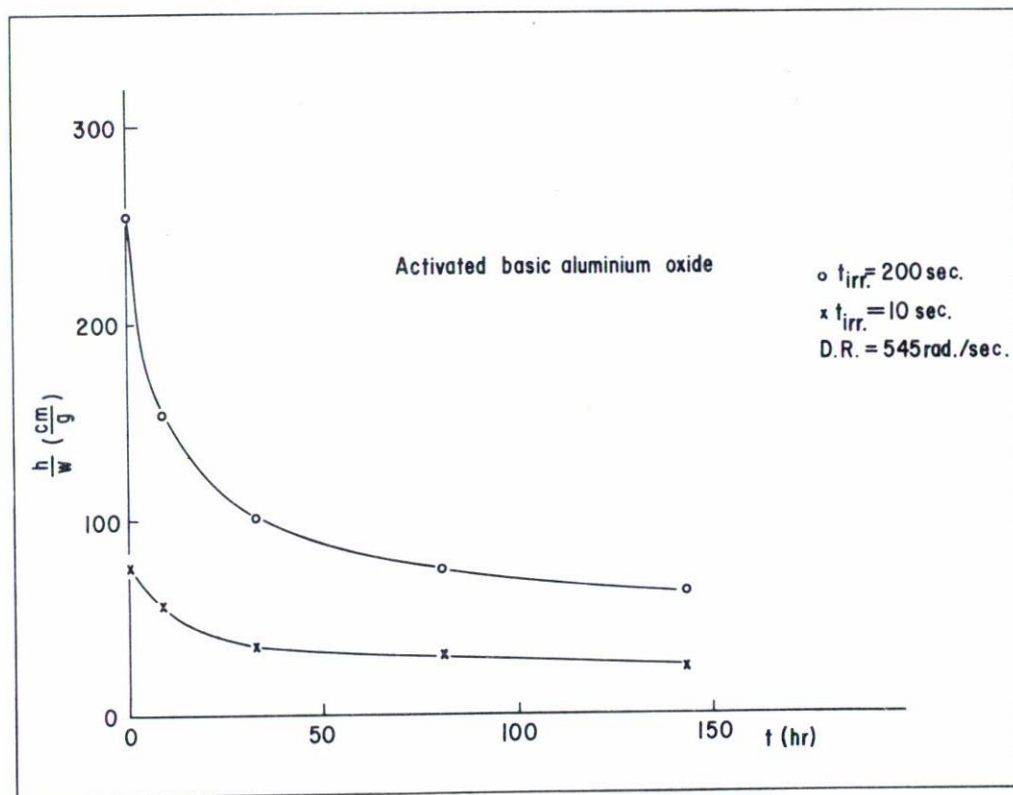


Fig. 2 Decay of the electron-induced paramagnetic species in activated basic aluminium oxide at room temperature.  $(b/w)$  represents the first derivative ESR line peak to peak height per mass unit. D.R. is the dose rate.



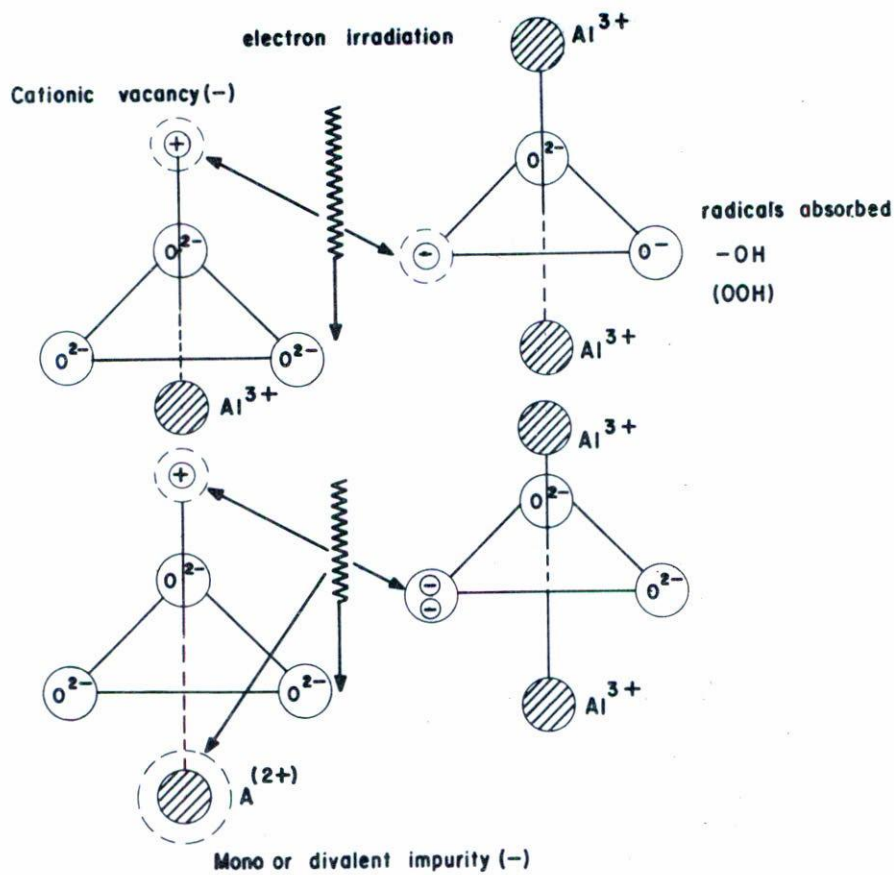


Fig. 3 Schematic representation of the electron-induced paramagnetic species in aluminium oxide catalysts, after Gamble<sup>8</sup>.

ation and an increase in intensity is also observed when the powder is subjected to electron irradiation, as can be seen in fig. 1.

In addition to the paramagnetic species found by Gamble<sup>8</sup> it is also possible that the ionization of the  $\bullet\text{OOH}$  and  $\bullet\text{OH}$  radicals absorbed in the aluminium oxide structure gives place to anionic vacancies and hydrogen atoms, which have been detected by ESR at low temperatures.

When the irradiated powder is maintained in air at room temperature, the ESR line intensity decreases, as can be seen in fig. 2, where the result for the basic oxide is plotted as an example. This annealing is due to the liberation of the trapped electrons and holes, followed by their recombination.

If we assume that Gamble's results for single crystals of aluminium oxide are valid for polycrystalline powder, the paramagnetic species are tentatively attributed to two types of centres: a trapped hole localized on an anion adjacent to a cation site (see fig. 3) which is deficient in positive charge, and an electron trapped at an anion vacancy. The cation site may be vacant or may contain a mono- or divalent substitutional impurity.

Annealing at room temperature involves only the transfer of charge rather than the elimination of defects, as is proved by the fact that the paramagnetic species can be restored again by irradiation after the annealing. If we suppose that there is only one process of transfer of charge, the annealing behaviour should give an exponential relation between the concentration of paramagnetic species and time, but this was not observed in the annealing.

Annealing was also observed at several temperatures, 50, 75, 100, 125 and 150°C and our results have been plotted in figures 4, 5 and 6. All measurements of this temperature annealing of the electron-induced ESR absorption were made for samples irradiated to 140 Krad, that is, in the saturation region. If we analyze the result, it is possible to observe that there are at least two different processes of temperature annealing, as indicated by the change in the slopes of the curves shown in the figures. The figure corresponding to the annealing behaviour of the irradiated acid oxide shows this change, as an example, indicated by lines A, B and C. It is also observed that the change is more pronounced at lower temperatures, e.g. 75°C, than at higher temperatures, e.g. 150°C. This

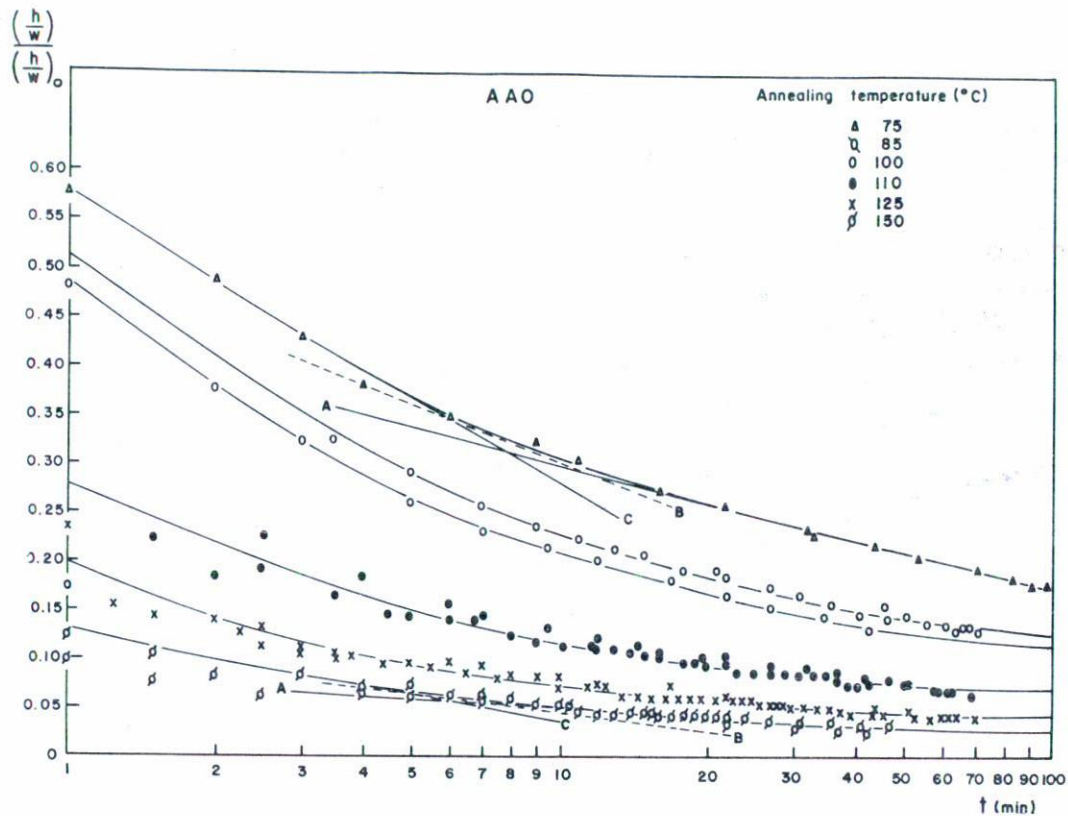


Fig. 4 Annealing temperature behaviour of the paramagnetic species induced by electron irradiation, at different temperatures.  $(h/w)_0$  and  $(h/w)$  are the relative concentrations of paramagnetic species, given by the peak to peak height of the first derivative of the ESR absorption line per mass unit, for times  $t_0$  and  $t$  respectively. The results shown are for the acid aluminium oxide powder.

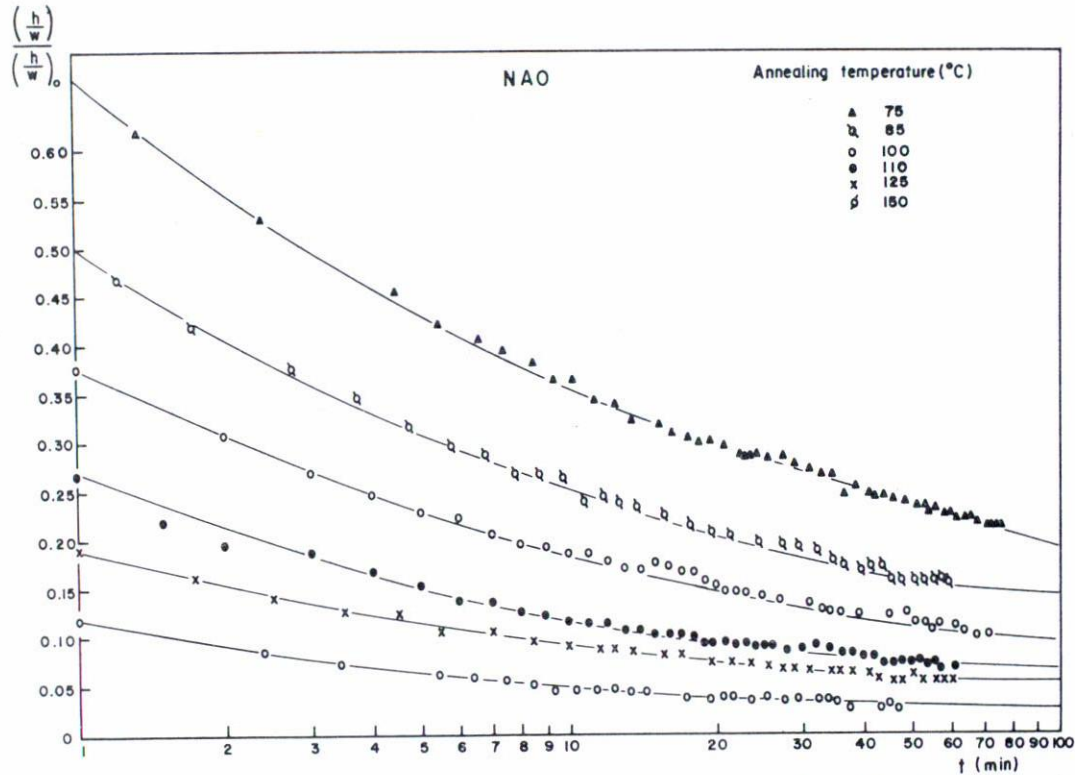


Fig. 5 Annealing temperature behaviour of the paramagnetic species induced by electron irradiation, at different temperatures.  $(b/w)_0$  and  $(b/w)$  are the relative concentrations of paramagnetic species, given by the peak to peak height of the first derivative of the ESR absorption line per mass unit, for times  $t_0$  and  $t$  respectively. The results shown are for the neutral aluminium oxide powder.

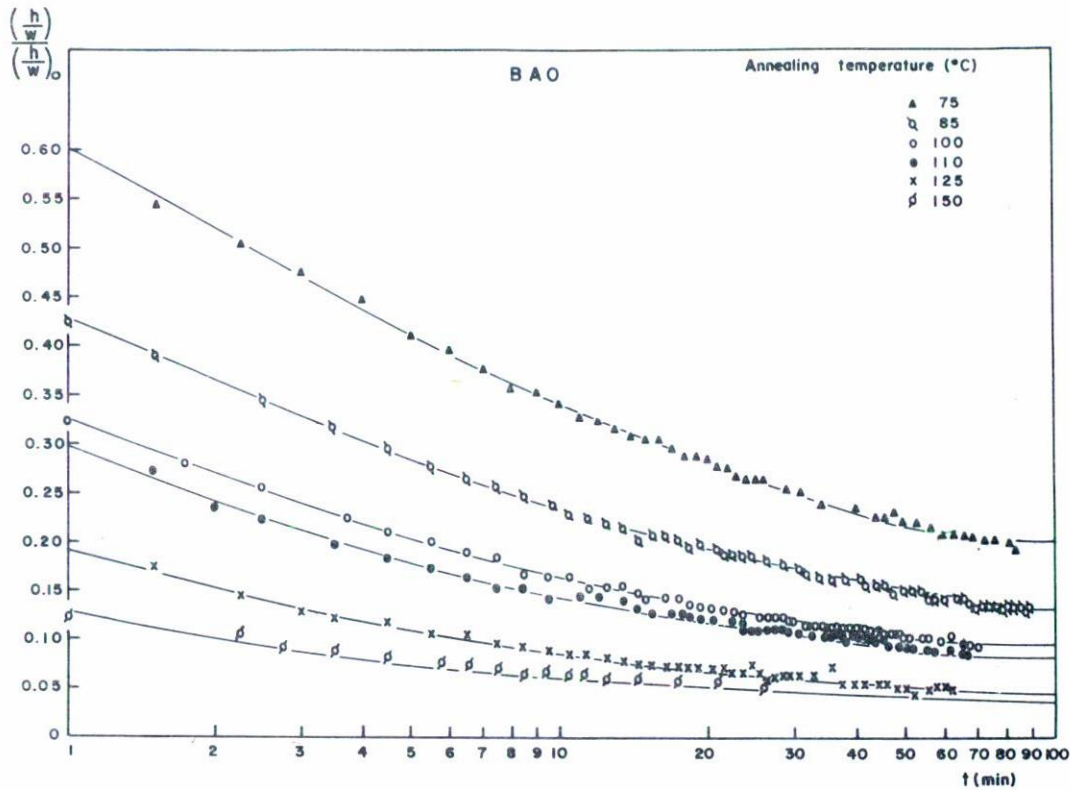


Fig. 6. Annealing temperature behaviour of the paramagnetic species induced by electron irradiation, at different temperatures.  $(h/w)_0$  and  $(h/w)$  are the relative concentrations of paramagnetic species, given by the peak to peak height of the first derivative of the ESR absorption line per mass unit, for times  $t_0$  and  $t$  respectively. The results shown are for the basic aluminium oxide.

suggests a temperature dependence of the annealing. For clarity, figure 5 presents simple annealing curves for 30 minutes treatment at each temperature indicated, from which it is possible to see that the temperature behaviour is different for two intervals, one from 60 to 100°C and another one from 100 to 150°C. This result suggests a dependence on the water content in the samples. It is interesting to point out that the mean activation energy for the total thermal recombination required for the process at annealing temperatures below 100°C, is higher than that required for the process at annealing temperatures higher than 100°C. These values are indicated in figure 5 and were calculated in the following way:

We assume that the total process of temperature annealing, a possible combination of several processes, can be described by the relation

$$(b/w) = (b/w)_0 \exp(-at) \quad (2)$$

where  $(b/w)_0$  and  $(b/w)$  are the relative concentrations of paramagnetic species, given by the peak-to-peak height of the first derivative of the ESR absorption line per mass unit, for times  $t_0$  and  $t$  respectively.  $a$  is a constant that is assumed equal to  $E_a/kT$ , where  $E_a$  is the activation energy,  $k$  Boltzmann's constant and  $T$  the annealing temperature.

If we take the log of the relation (2), we have

$$\log(b/w) = \log(b/w)_0 - at$$

so in order to obtain the values of  $a$ , we calculated, from the experimental values (figures 4, 5 and 6), the least squares equations for each temperature, and combining these values with different temperatures, the following results were obtained:

Temperature interval (°C)	Mean total activation energy (eV)		
	AAO	BAO	NAO
< 100	0.0667	0.0634	0.0655
100 - 150	0.0735	0.0636	0.0688

Further analysis must be done of the change in the slopes of annealing behaviour curves. However, any analysis should keep in mind that Gamble has shown that the number of holes is reduced faster than the number of electrons.

Bartram<sup>17</sup> indicates that an anion vacancy in aluminium oxide constitutes a deep trap for one or two electrons, so, if the annealing is accomplished by the liberation of holes trapped in cation vacancies, the holes would tend to be repelled by anion vacancies with one trapped electron, which are positive centres, and consequently the number of trapped holes and single trapped electrons would tend to equalize as annealing progressed, which could explain the lines A, B and C in figures 4 to 6.

Polak<sup>18</sup> has suggested that the transfer of energy from the catalyst to adsorbed molecules explains the increment of G values in the heterogeneous radiolysis, and that in some way it is connected with the recombination of trapped electron-holes.

We have been examining the problem of energy transfer in heterogeneous radiation catalysis in aluminium oxide with respect to excitation, ionization and recombination of paramagnetic species formed by irradiation. However, there is evidence of effects other than the catalytic one. The role of stable defects, with respect to displacement, vacancies, temperature peaks, photons emitted in recombination processes and some specific surface effects, remains obscure. More study of radiation-induced catalytic processes is necessary for elucidating these problems. There is reason to believe that efforts in this direction will be justifi-

fied both from the theoretical and from a practical point of view since these processes may open up wide possibilities for use of nuclear and other powerful radiations in the chemical industry.

#### ACKNOWLEDGMENTS

The authors acknowledge Carlos Ruiz Mejía and Héctor Riveros Rotgé for their helpful comments and discussions; Octavio Cano C., for the X-ray spectrographic analysis; J. Osorno, for his help in carrying out the numerical calculations using the facilities at Centro de Cálculo Electrónico, UNAM; A.A. Valladares C. and Mrs. Mary Ann M. de Valladares for proof-reading the manuscript.

#### REFERENCES

1. R.F. Coekelbergs, et al. *Advan. Catalysis*, **13**, 55 (1962).
2. I.A. Kolbanovskii, et al. *Proc.Symp.Radiat.Chem. of Polymers*, Moscow (1965).
3. S.H. Cheek; et al. *J. Phys.Chem.*, **62**, 1475 (1958).
4. V.I. Vladimirova, *Dokl. Akad. Nauk SSSR*, **164**, 361 (1965).
5. V.I. Vladimirova, *idem*, **148**, 101 (1963).
6. P.J. Dyne, et al. *Can.J.Chem.*, **39**, 2381 (1961).
7. V.B. Kazanskii, et al. *Zhur.Fiz.Khim.* **34**, 477 (1960).
8. F.T. Gamble, et al. *Phys.Rev.* **134**, A589 (1964).
9. G.J.K. Acres, et al. *J. Catalysis* **4**, 12 (1965).
10. R.T. Cox, *Phys.Letters* **21**, 503 (1966).
11. R.H. Bartram, et al. *US AEC NYO-2047-36* (1966).
12. R.P. Thorne, et al. *Proc.Brit.Ceram.Soc.* **7**, 439 (1967).
13. S.A. Reyes L., et al. *Rev.Mex.Fís.* **16**, 31 (1967).
14. A.T. Nelms, *US National Bureau of Standards, Circular 577* (1956).
15. T. Henriksen, et al, *Radiat. Res.* **6**, 415 (1956).
16. P.H. Emmett, et al. *J.Phys.Chem.* **66**, 921 (1962).
17. R.H. Bartram, et al. *Phys.Rev.* **139**, (3A) 941 (1965).



18. L.S. Polak, et al. *Pure Appl. Chem.* **10**, 441 (1965).
19. J. Reyes L., *Segunda Conferencia Interamericana de Radioquímica*, México D.F., Abril (1968).

